JACS Au
AN OPEN ACCESS JOURNAL OF THE AMERICAN CHEMICAL SOCIETY

pubs.acs.org/jacsau

Article

Ortho Effects of Tricarboxylate Linkers in Regulating Topologies of Rare-Earth Metal−Organic Frameworks

Fugang Li,[‖] Kun-Yu Wang,[‖] Zhengyang Liu, Zongsu Han, Dacheng Kuai, Weidong Fan,* Liang Feng, Yutong Wang, Xiaokang Wang, Yue Li, Zhentao Yang, Rongming Wang, Daofeng Sun,* and Hong-Cai Zhou*

Cite This: *JACS Au* 2023, 3, 1337−1347

Read Online

ACCESS | Metrics & More | Article Recommendations | Supporting Information

ABSTRACT: A linker design strategy is developed to attain novel polynuclear rare-earth (RE) metal−organic frameworks (MOFs) with unprecedented topologies. We uncover the critical role of ortho-functionalized tricarboxylate ligands in directing the construction of highly connected RE MOFs. The acidity and conformation of the tricarboxylate linkers were altered by substituting with diverse functional groups at the ortho position of the carboxyl groups. For instance, the acidity difference between carboxylate moieties resulted in forming three hexanuclear RE MOFs with novel (3,3,3,10,10)-c **wxl**, (3,12)-c **gmx**, and (3,3,3,12)-c **joe** topologies, respectively. In addition, when a bulky methyl group was introduced, the incompatibility between the net topology and ligand conformation guided the co-appearance of hexanuclear and tetranuclear clusters, generating a novel 3-periodic MOF with a (3,3,8,10)-c **kyw** net. Interestingly, a fluoro-functionalized linker prompted the formation of two unusual trinuclear clusters and produced a MOF with a fascinating (3,8,10)-c **lfg** topology, which could be gradually replaced by a more stable tetranuclear MOF with a new (3,12)-c **lee** topology with extended reaction time. This work enriches the polynuclear clusters library of RE MOFs and unveils new opportunities to construct MOFs with unprecedented structural complexity and vast application potential.

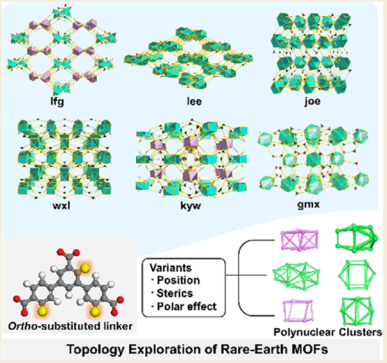

KEYWORDS: *metal−organic framework, topology, rare earth, ortho effect, high connectivity*

INTRODUCTION

Metal−organic frameworks (MOFs) have fueled considerable interest from researchers due to their remarkable potential for advanced applications, such as gas separation,[1−4] energy storage,[5−10] water harvesting,[11−13] and carbon capture.[14−18] As a supramolecular assembly, MOFs consist of periodically interlinked metal-containing nodes and organic linkers to give exceptional porosity and tunable topologies.[19−25] Therefore, rational linker design is an effective approach to regulate MOF topologies, which can be altered by tuning the substituents, sizes, geometries, and symmetry of the organic linkers.[26] For instance, the combination of a linear terephthalate (BDC) and a square paddlewheel cluster usually leads to MOF-2 as a two-dimensional (2D) **sql** net. Yaghi and co-workers successfully assembled the paddlewheel clusters into a three-dimensional (3D) **nbo** net by employing a sterically hindered o-Br-BDC linker.[27] Later, Yaghi and Furukawa et al., systematically adjusted the substituent locations and linker symmetry in the 4,4′-biphenyldicarboxylate (BPDC) and attained a series of paddlewheel-based frameworks ranging from zero-dimensional (0D) to 3D.[28] This design strategy was further introduced into the Zr-MOFs by our group, in which a methyl-functionalized BPDC linker was designed to construct a **bcu** MOF named PCN-700 with unsaturated Zr_6 clusters, rather than the **fcu** net observed in UiO-67 (PCN = porous coordination network; UiO = University of Oslo).[29−33] These practices in exploring MOF topologies significantly enriched the structural library of MOFs, empowering the functional materials with huge application potential.

Recently, rare-earth (RE) MOFs have drawn wide attention owing to their diverse structures and versatility. The highly adaptable coordination modes of RE elements allow for multiple coordination directionality of carboxylate ligands, facilitating the occurrence of polynuclear clusters with various connectivity and geometries. Yet, the observation of polynuclear RE clusters was usually viewed as synthetic serendipity at the early stage of MOF research.[34,35] Beyond aforementioned, the varieties of reported RE polynuclear clusters are relatively limited in MOFs, given the fact that most reported RE MOFs are based on mono-/di-nuclear clusters or rod-shaped RE-chains.[34,36,37] The scarcity of RE polynuclear clusters can be attributed to their dynamic nature, making

Received: November 19, 2022
Revised: March 19, 2023
Accepted: March 20, 2023
Published: April 26, 2023

https://doi.org/10.1021/jacsau.2c00635
JACS Au 2023, 3, 1337−1347

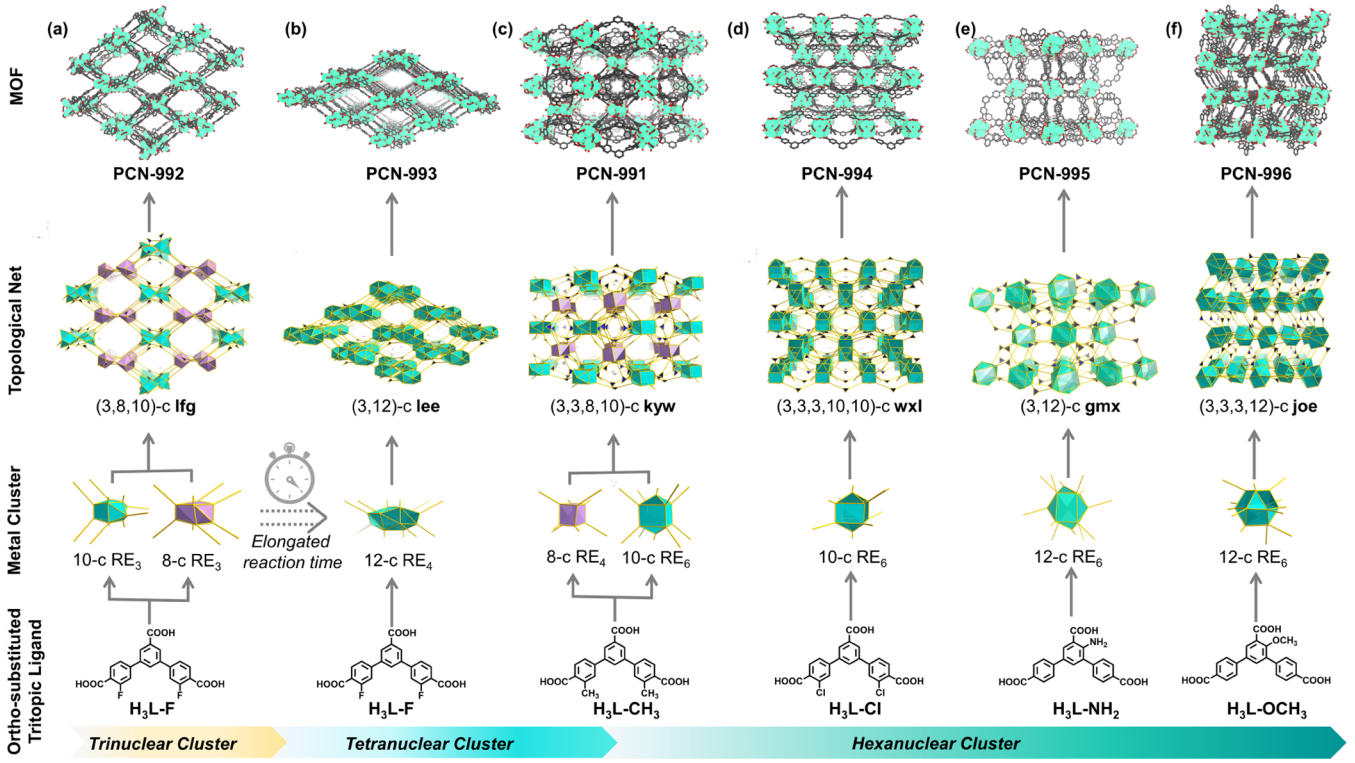

Figure 1. Illustration of diverse topologies in highly connected RE MOFs based on ortho-substituted tricarboxylate ligands. (a) Employment of a fluoro-functionalized linker H_3L−F induced the formation of PCN-992(Eu) featuring a novel (3,8,10)-c **lfg** net based on 8-c and 10-c RE_3 clusters. (b) PCN-992(Eu) was replaced by PCN-993(Eu) by elongated reaction time, which adopts a (3,12)-c **lee** net with 12-c RE_4 clusters. (c) Methyl-functionalized linker H_3L−CH_3 resulted in the co-appearance of 10-c RE_6 clusters and 8-c RE_4 clusters, which were assembled into PCN-991(Eu) with a new (3,3,8,10)-c **kyw** net. (d) Chloro-functionalized linker H_3L−Cl led to the discovery of a (3,3,3,10,10)-c **wxl** net with the 10-c RE_6 clusters. (e) Amino-functionalized linker H_3L−NH_2 formed PCN-995(Eu) with a two-nodal (3,12)-c **gmx** net. (f) Combination of a methoxyl-functionalized linker H_3L−OCH_3 and 12-c RE_6 clusters generated a highly connected (3,3,3,12)-c **joe** net. The metal clusters, C atoms, and O atoms are represented in turquoise, dark gray, and red, respectively. H atoms are omitted for clarity.

them unattainable during MOF synthesis. Herein, compatible coordination spheres are required to stabilize the RE clusters. For instance, Rosi and co-workers constructed a series of RE_4-based MOFs with an amino group-functionalized carboxylic acid.[38] Notably, the ortho-amino group structurally directs the formation of the octahedral 6-c RE_4 cluster.[39−47] Similarly, Eddaoudi and co-workers employed ortho-fluorinated ditopic linkers to prepare **fcu** MOFs with fully coordinated 12-c RE_6 clusters.[48] They concurrently observed the occurrence of 8-c RE_6 and 12-c RE_9 clusters in a (3,8,12)-c **pek** MOF with tritopic ligands, in which the formation of RE_9 clusters was attributed to the incompatibility between the net and ligand geometry.[49] We also intentionally decreased the symmetry of a series of tri-/tetracarboxylate linkers and attained RE_9-based MOFs with cluster connectivity numbers of 12, 14, or 18.[50] Nevertheless, it remains a challenge to construct highly connected RE MOFs bearing unprecedented polynuclear clusters and new topologies through rational linker design despite recent progress.

Ortho effect is a fundamental phenomenon widely observed in organic chemistry, which significantly affects the acidity and reactivity of aromatic compounds, especially aromatic carboxylic acid[51,52] (Figure S1). Although most reported MOFs are based on aromatic carboxylate linkers, the significance of ortho effect in regulating topologies of RE MOFs is grossly underestimated. Herein, we chose a tritopic linker as the prototype and deliberately introduced ortho-substituents into the central or the peripheral phenyl rings (Figure 1). The ortho-substituents will force adjacent carboxylates into a specific dihedral angle with the phenyl rings and affect the carboxylate acidity, forming unusual polynuclear RE clusters. For instance, the fluoro-functionalized linker H_3L−F will prompt the formation of two unusual trigonal trinuclear clusters, 8-connected RE_3 and 10-connected RE_3, and produce another layered mixed-cluster MOF with a new (3,8,10)-c **lfg** topology (Figure 1a). More interestingly, while extending the reaction time, the RE_3-based MOF can be gradually replaced by a more stable MOF with a new (3,12)-c **lee** topology, consisting of unusual 12-connected RE_4 clusters (Figure 1b). This transformation is unprecedented in RE MOFs, attributed to the incompatibility in the linker geometry and coordination requirements of the clusters in the initial MOF. Besides, the H_3L−CH_3 linker with bulky methyl groups guides the co-appearance of octahedral hexanuclear RE_6 clusters and rare diamondoid tetranuclear RE_4 clusters (Figure 1c), generating a highly porous mixed-cluster MOF with an engaging (3,3,8,10)-c **kyw** topology. In addition, some other layered MOFs are discovered by using hexanuclear RE_6 clusters and linkers functionalized with chloro, amino, or methoxy, demonstrating new (3,3,3,10,10)-c, (3,12)-c, or (3,3,3,12)-c topologies (Figure 1d−f).

https://doi.org/10.1021/jacsau.2c00635
JACS Au 2023, 3, 1337−1347

RESULTS AND DISCUSSION

Design of Ortho-Functionalized Tricarboxylic Linkers

A tricarboxylate linker [1,1′:3′,1″-terphenyl]-4,4″,5′-tricarboxylic acid (H_3L−H) was selected as the prototype, consisting of two peripheral phenyl rings and one central phenyl ring. The two peripheral phenyl rings represent an angle of 120°. Previous studies indicate that the H_3L−H could afford MOFs with (3,3,18)-c **ytw** topology, in which a rare 18-connected nonanuclear RE cluster was discovered.[50,53] In this work, ortho positions to H_3L−H's carboxyl were substituted with various functional groups to investigate the role of ortho effects in the MOF topology regulation. Given that there are three variables in the linker design, namely, substitution position, steric hindrance, and electronic effect, fluoro, chloro, and methyl were deliberately introduced to the 3 and 3″ positions of H_3L−H, leading to H_3L−F, H_3L−Cl, and H_3L−CH_3. Moreover, the 4′ position of H_3L−H can be functionalized with amino and methoxyl groups, resulting in the linkers H_3L−NH_2 and H_3L−OCH_3 (Figure 1).

Synthesis and Structural Description of a Mixed-Cluster MOF

A solvothermal reaction between H_3L−CH_3 and $Eu(NO_3)_3\cdot 6H_2O$ produced colorless crystals, named as PCN-991(Eu), in the presence of 2-fluorobenzoic acid (2-FBA). The utilization of 2-FBA can facilitate the in-situ formation of hexanuclear RE_6 clusters,[48,54−58] which can be interlinked and extended to afford 3-periodic networks. Interestingly, according to single-crystal X-ray diffraction (SCXRD) studies, PCN-991(Eu) consists of both 10-c hexanuclear clusters $[RE_6(\mu_3\text{-}OH)_8(COO)_{10}]$ and 8-c tetranuclear clusters $[RE_4(\mu_3\text{-}O)_2(COO)_8]$ (Figure 1c, Table S1). Note that the 10-c RE_6 cluster can be regarded as an elongated square bipyramid, a Johnson solid labeled as J_{15}, while the 8-c RE_4 cluster can be simplified into a cube (Figure S2d,e). The two kinds of nodes are interlinked by tritopic ligands to attain a new 3-periodic (3,3,8,10)-c **kyw** net with a point symbol of $\{4^2\cdot6\}_4\{4^3\}_2\{4^6\cdot6^6\cdot8^{14}\cdot10^2\}\{4^8\cdot6^{20}\cdot8^{13}\cdot10^4\}$ as determined by ToposPro.[59,60]

Further structural analysis revealed that the mixed-cluster PCN-991(Eu) was constructed via a supramolecular building layer approach.[49,61] The tritopic ligand can form a 2-c moiety, [1,1′:3′,1″-terphenyl]-4,4″-dicarboxylate (H_2TDC), after eliminating the carboxyl on the central phenyl ring. The RE_6 clusters were bridged by the TDC, thus leading to a 2D double cross-linked **sql** net (Figure 2a). Specifically, the PCN-991(Eu) features an AAA stacking of **sql** layers, when merely considering the TDC moieties, consisting of RE_6 clusters bridged with four adjacent clusters through eight TDC moieties. The central phenyl rings of TDC moieties point the rectangular pores of **sql** nets inward, inducing the RE_4 cluster to intercalate the adjacent two **sql** layers, in virtue of the incompatibility between the **sql** net and the RE_6 clusters (Figure 2b). Herein, the (3,3,8,10)-c **kyw** net consists of two layers, namely, a double cross-linked **sql** layer and a periodic array of 8-c RE_4 clusters (Figure 2c). In 2015, Eddaoudi and co-workers reported **pek** MOFs featuring 12-c RE_9, 8-c RE_6 clusters, and 3-c ligands.[49] Herein, PCN-991(Eu) represents a rare MOF composed of two polynuclear clusters, which can be regarded as a complementary case for the **pek** net.

The powder X-ray diffraction (PXRD) patterns show that the crystallinity of PCN-991(Eu) can be maintained at a broad pH range from 4 to 10, demonstrating the framework's chemical stability (Figures S8 and S9). The thermal stability of

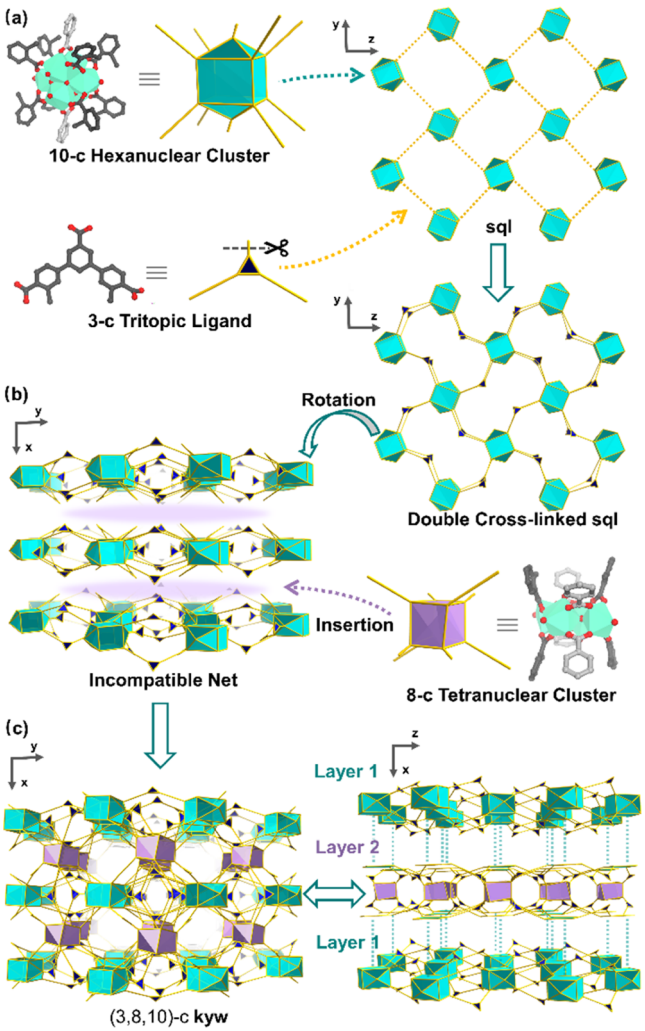

Figure 2. Schematic of PCN-991(Eu) with the new (3,3,8,10)-c **kyw** topology. (a) Elongated square bipyramid, representing the 10-c RE_6 cluster, can be interconnected by H_3L−CH_3 to generate a double cross-linked **sql** net. (b) Network incompatibility prompted the formation of the C_4-symmteric 8-c RE_4 cluster. (c) RE_4 clusters served as pillars for the **kyw** net.

PCN-991(Eu) was tested through thermal gravimetric analysis (TGA) (Figure S15). Additionally, nitrogen sorption tests demonstrated that PCN-991(Eu) features a high Brunauer−Emmett−Teller (BET) surface area of 1179 m^2/g and micropores at 6, 8, and 11 Å (Figures S20−S22). The application potential of PCN-991(Eu) was evaluated, which featured moderate CO_2/CH_4 selectivity (Figure S26).

Synthesis and Structural Description of RE_6-Based MOFs

Functionalizing the peripheral phenyl rings of the tritopic linker with chloride groups can produce the linker H_3L−Cl. The combination of deprotonated L-Cl and $[RE_6(\mu_3\text{-}OH)_8(COO)_{10}]$ leads to the formation of PCN-994(Eu) with a new (3,3,3,10,10)-c **wxl** net (Table S2). The RE_6 clusters can be viewed as an elongated square bipyramid (J_{15}), identical to the 10-c RE_6 observed in PCN-991(Eu) (Figure S1e). One RE_6 cluster is bridged with six neighboring clusters through the 3-c L-Cl (Figure 3a). Furthermore, an ABAB stacking of two layers is observed in PCN-994(Eu) (Figure 3b). Specifically, the **wxl** net can be separated into stacked one-dimensional (1D) supramolecular ribbons when considering

https://doi.org/10.1021/jacsau.2c00635
JACS Au 2023, 3, 1337−1347

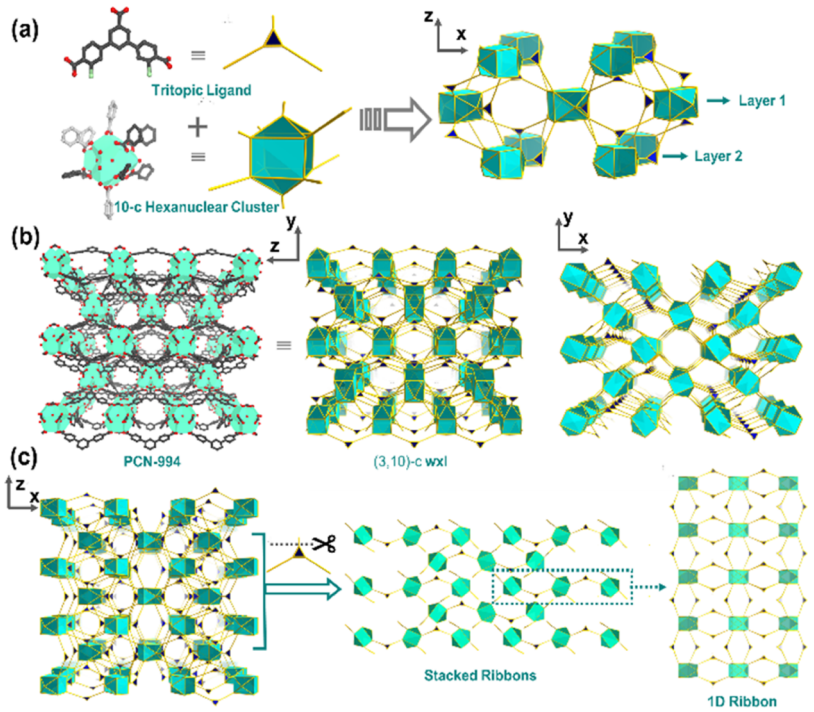

Figure 3. Structural illustration of PCN-994(Eu) with (3,3,3,10,10)-c **wxl** topology. (a) Elongated square bipyramids, representing 10-c RE_6 clusters, were interlinked through the tritopic ligands to form a **wxl** net. (b) Layered packing of RE_6 clusters was observed in PCN-994(Eu). (c) (3,3,3,10,10)-c **wxl** net can be viewed as a close stack of 1D supramolecular ribbons when cleaving one carboxylate of the tritopic ligand.

the L-Cl as a TDC moiety. The supramolecular ribbon is a one-periodic array of three RE_6 clusters (Figure 3c). Ribbons are closely packed along the *z* axis, and the matched symmetry between adjacent ribbons ensures the formation of the ABAB stacking **wxl** net (Figure S7).

When the $H_3L{-}NH_2$ with amino group at the 4′-position serves as the ligand, a MOF named PCN-995(Eu) featuring a (3,12)-c **gmx** net can be attained. According to crystallographic studies, PCN-995(Eu) consists of RE_6 clusters connecting with 12 neighboring clusters (Figure 4a). A disorder of ligands is observed in the crystal structure, which is originated from the *C*2/*c* space group. In addition, the RE_6 clusters are interlinked through doubly cross-linked ligands to afford a **sql** net (Figure 4b,c). Note that the **sql** nets are packed through ABAB mode, leading to the 2-nodal **gmx** net with a point symbol of $\{4^{12}{\cdot}6^{38}{\cdot}8^{16}\}\{4^3\}_4$.

The utilization of 4′-substituted $H_3L{-}OCH_3$ induced the formation of PCN-996(Eu) with $[RE_6(\mu_3\text{-}OH)_8(COO)_{12}]^{2-}$ clusters, crystallized in the monoclinic space group *P*21/*n* (Figure 5a, Table S2). PCN-996(Eu) demonstrates a BET surface area of 891 m^2/g with a pore size of 7.6 Å (Figures S23−S25). When viewing the carboxylates as the vertices, the 12-c RE_6 cluster can be represented as a cuboctahedron, an Archimedean solid (Figure S1f). Overall, PCN-996(Eu) features a (3,3,3,12)-c **joe** topology with a point symbol of $\{4^{16}{\cdot}6^{34}{\cdot}8^{16}\}\{4^2{\cdot}6\}_2\{4^3\}_2$. Specifically, the **joe** net can be converted into AAA stacking layers after removing one peripheral carboxylate group of $H_3L{-}OCH_3$, in which the RE_6 clusters are double cross-linked to afford a **sql** net (Figure 5b). Compared with the (3,12)-c **gmx** net, one RE_6 cluster connects nine adjacent clusters through one or three $H_3L{-}OCH_3$.

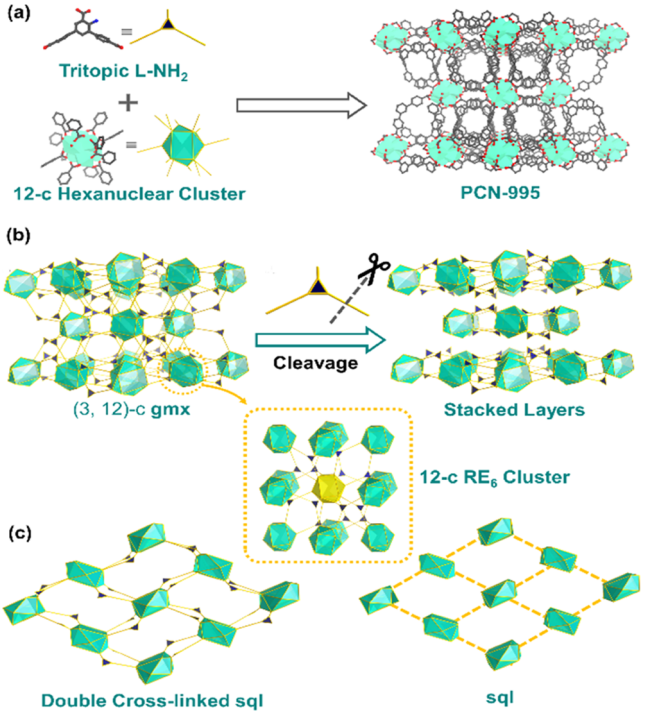

Figure 4. Structural illustration of PCN-995(Eu) with (3,12)-c **gmx** topology. (a) Cuboctahedron represents the 12-c RE_6 cluster, and the triangle represents the 3-c $H_3L{-}NH_2$ ligand. (b) 12-c RE_6 cluster, labeled in yellow, is bridged with 12 adjacent clusters, leading to a layered structure. (c) **gmx** net can be simplified into stacked double cross-linked **sql** nets.

Phase Transformation between RE_3- and RE_4-Based MOFs

A unique phase transformation was observed in the solvothermal reaction between 3,3″ functionalized 3-c $H_3L{-}$

https://doi.org/10.1021/jacsau.2c00635
JACS Au 2023, 3, 1337−1347

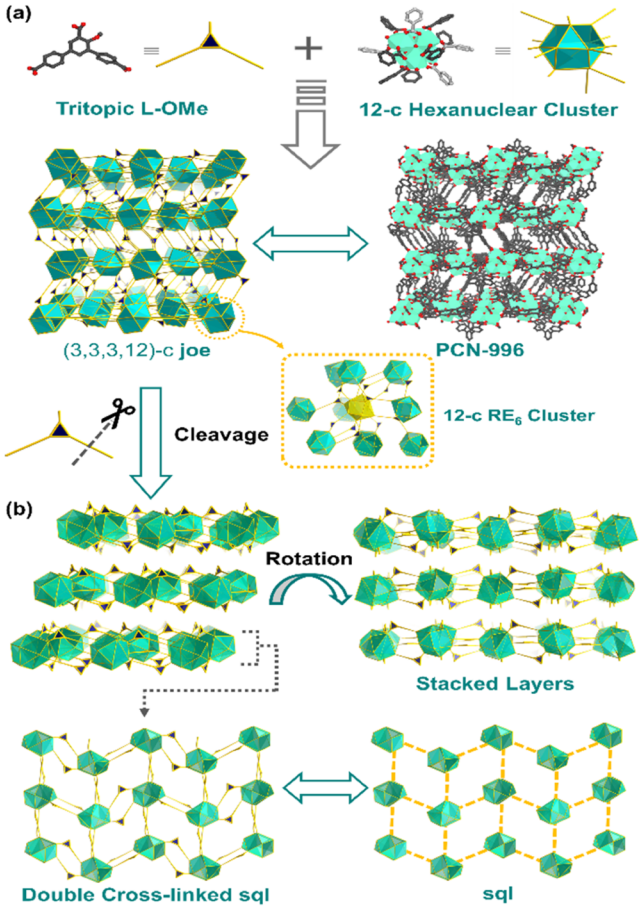

Figure 5. Structural illustration of PCN-996(Eu) with (3,3,3,12)-c **joe** topology. (a) Cuboctahedron represents the 12-c RE_6 cluster, and the triangle represents the 3-c H_3L−OCH_3 ligand. (b) Double cross-linked RE_6 **sql** nets are closely packed with each other to give the (3,3,3,12)-c **joe** topology.

F and $Eu(NO_3)_3{\cdot}6H_2O$ by varying the reaction time. Colorless rod-shaped crystals were observed after 36 h, named PCN-992(Eu). Interestingly, PCN-992(Eu) was replaced by some yellowish crystals, PCN-993(Eu), when extending the reaction time to 72 h (Figure 6). The two MOFs feature distinct RE clusters and topologies. For instance, the PCN-992(Eu) is composed of two kinds of clusters, 8-c $[RE_3(\mu_3\text{-OH})(COO)_8]$ and 10-c $[RE_3(\mu_3\text{-OH})(COO)_{10}]^{2-}$. Topologically, the 8-c RE_3 cluster can be viewed as a snub-disphenoid, a Johnson solid labeled as J_{84} (Figure S1a). The 10-c RE_3 cluster is represented as an arrowhead-tetradecahedron generated by augmenting two vertices to the middle of the snubdsphenoid (Figure S1b). ^{1}H NMR spectrum indicates that dimethylamine cations serve as the counter cations to balance the negative charge of integral framework (Figure S46). Trinuclear clusters are common for d-block metal-based MOFs.[62−71] However, only a limited number of RE_3 clusters have been reported, most of which feature linear or bent geometries.[72−76] To our knowledge, one rare example of trigonal prismatic RE_3 clusters was observed in a MOF named JXNU-3 composed of 15-c nonanuclear and 9-c trinuclear clusters.[77] Han, Gu, and co-workers reported several robust RE MOFs bearing 6-c trinuclear clusters in 2017.[78] Notably, it is challenging to tailor the coordination sphere to stabilize trigonal prismatic RE_3 clusters in coordination complexes, usually requiring chelating or macrocyclic auxiliary ligands.[79−84] Interestingly, the chemical structures of the two $[RE_3(\mu_3\text{-OH})(COO)_8]$ and $[RE_3(\mu_3\text{-OH})(COO)_{10}]^{2-}$ clusters in PCN-992(Eu) are pretty similar, in both of which the three RE ions feature coordination numbers of 8, 8, and 9, respectively, bridged by one μ_3-O atom and six μ_2-COO groups. Due to the high adaptability of RE-carboxylate coordination bonds, the 8-c RE_3 cluster consists of eight capping carboxylate groups, while the 10-c RE_3 cluster is surrounded by eight bidentate and two unidentate carboxylate groups (Figure S4). Each 10-c RE_3 cluster is connected to two 10-c RE_3 and six 8-c RE_3 through 3-c ligands, giving a (3,8,10)-c **lfg** net with a point symbol of $\{4^{16}{\cdot}6^4{\cdot}8^{25}\}\{4^2{\cdot}6\}_2\{4^3\}_4\{4^8{\cdot}6^4{\cdot}8^{15}{\cdot}10\}$ (Figure 7a). When viewed along the *y* axis, the **lfg** net can be divided into four different layers, in which the layers 1 and 3 and layers 2 and 4 are inverse to each other (Figure 7b,c). To further investigate the topology, one peripheral ring of the H_3L−F is assumed to be cleaved, and the **lfg** net is converted into two sets of zigzag supramolecular chains, composed of doubly or quadruply cross-linked RE_3 clusters (Figure 7c−f). The interlinked zigzag chains form the **lfg** net with rhomboid channels.

Furthermore, a 12-c $[RE_4(\mu_3\text{-OH})_2(COO)_{12}]^{2-}$ cluster was observed in the thermodynamic product PCN-993 during the synthesis, where the integral charge of the anionic framework is balanced by dimethylamine cations (Figure S48). The 12-c RE_4 cluster can be represented by the sphenomegacorona, another Johnson solid labeled as J_{88}, with 12 vertices and 18 faces (Figure S1c). The four RE ions in the 12-c cluster are arranged in a rhombic manner, bridged by two μ_3-O atoms. Notably, the $[RE_4(\mu_3\text{-OH})_2(COO)_{12}]^{2-}$ cluster can be transformed from the $[RE_3(\mu_3\text{-OH})(COO)_8]$ by augmenting one RE metal and four capping carboxylates (Figure S5). Although similar rhombic RE_4 clusters have been reported in several coordination complexes and frameworks, the 12-c $[RE_4(\mu_3\text{-OH})_2(COO)_{12}]^{2-}$ represents one RE_4 cluster with the highest connectivity number to the best of our knowledge.[35,85−87]

In the PCN-993(Eu) with the orthorhombic space group *Fddd*, each RE_4 cluster is connected with eight adjacent RE_4 clusters through the 3-c H_3L−F ligands, affording a (3,12)-c **lee** net with a point symbol of $\{4^{22}{\cdot}6^8{\cdot}8^{32}{\cdot}10^4\}\{4^3\}_4$ (Figure 8a). When cleaving the carboxylate on the central phenyl ring and converting the 3-c H_3L−F into the TDC moiety, the RE_4 clusters will be assembled into a double cross-linked **sql** layer. (Figure 8c). The two neighboring **sql** nets can be packed closely and intercalated to give an ABAB stacking due to the compatibility between the layers (Figure 8b). Moreover, the (3,12)-c **lee** net can be eliminated into an ABAB stacking of **hcb** layers by removing one peripheral phenyl ring of the 3-c H_3L−F (Figure S5). The **hcb** net is cross-linked by quadruple H_3L−F ligands to form hexagonal pores. The adjacent **hcb** nets can be fused to generate hexagonal channels (Figure S6). Overall, both rhombic and hexagonal channels are present in the (3,12)-c **lee** net.

Formation Mechanism of Diverse Topologies

The structural diversity of RE MOFs can be attributed to the highly adaptable coordination modes of the RE ions, allowing multiple coordination directionality of carboxylate ligands. As a result, a series of polynuclear clusters with various connectivity and geometries have been attained, leading to diverse MOF topologies. In coordination complexes, structures of lanthanide−oxo clusters profoundly depend on factors such as ligand types, auxiliary ligands, metal types, and reaction conditions.[40,88−91] Our work suggests that the ortho functionaliza-

https://doi.org/10.1021/jacsau.2c00635
JACS Au 2023, 3, 1337−1347

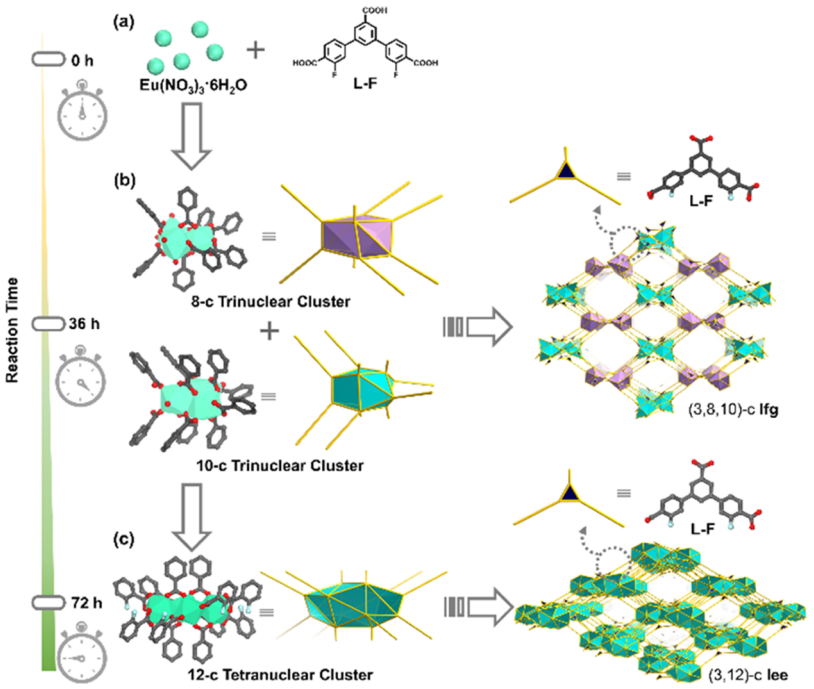

Figure 6. (a) Use of fluoro-functionalized H_3L−F ligand induced the formation of two RE MOFs with different reaction time. (b) PCN-992(Eu) with (3,8,10)-c **lfg** topology appeared after 36 h, consisting of rare 8-c and 10-c RE_3 clusters. (c) After 72 h, the PCN-992(Eu) would be replaced by PCN-993(Eu) with the highly connected (3,12)-c **lee** topology, which was based on 12-c RE_4 clusters.

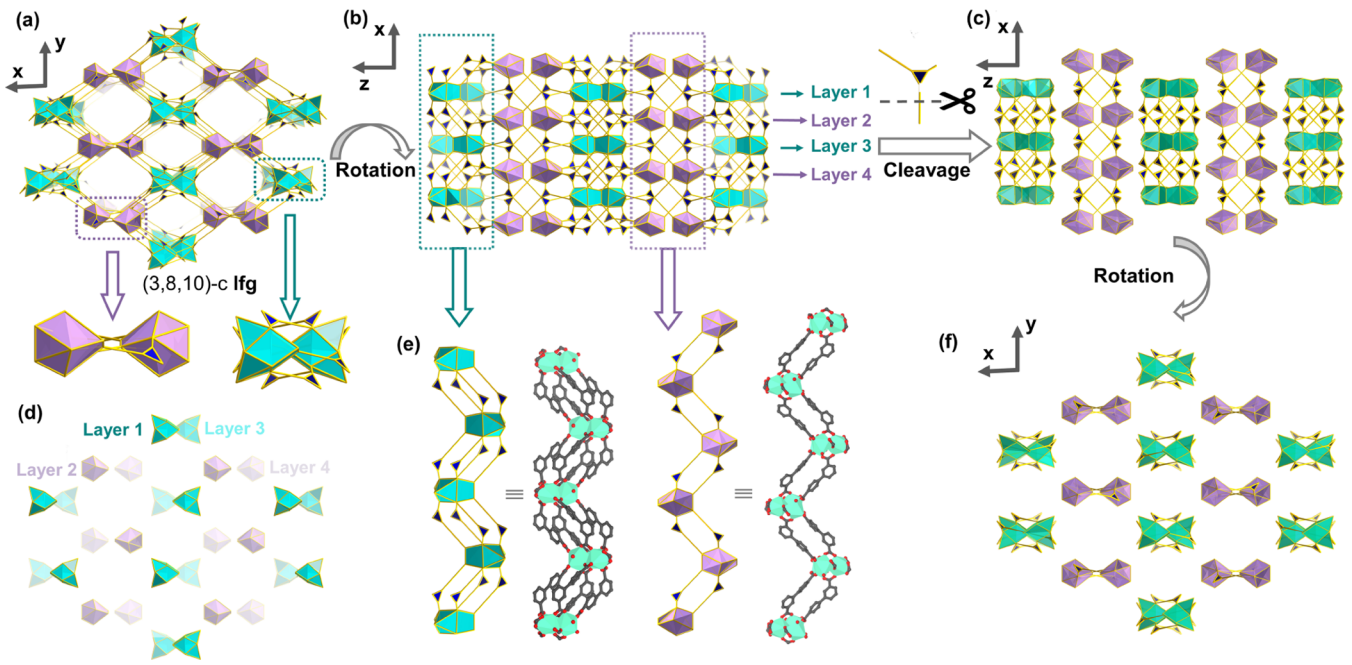

Figure 7. Structural illustration of PCN-992(Eu) with the (3,8,10)-c **lfg** topology. (a) Lavender snub-disphenoid represents the 8-c RE_3 cluster, and the turquoise arrowhead-tetradecahedron represents the 10-c RE_3 cluster. (b, d) **lfg** net contains four different layers along the *x* axis, in which the layers 1 and 3, and layers 2 and 4 are inverse to each other. (c, e, f) **lfg** net can be divided into two zigzag chains when cleaving one carboxylate of the H_3L−F ligand.

tion in tricarboxylate linkers contributes to the formation of diverse metal−oxo clusters, which are essential building blocks constructing the overall frameworks. Herein, we investigated how the altered ortho functionalization regulates the RE cluster structures and framework topologies.

The presence of functional groups at ortho position can significantly affect the acidity of the carboxyl group in benzoic acid, which can be attributed to the electronic effects and steric hindrance (Figure S28). Herein, introducing ortho functional groups into the prototype ligand, [1,1′:3′,1″-terphenyl]-4,4″,5′-tricarboxylic acid, will not only change the overall conformation but also bring acidity difference between the carboxylates. To confirm our hypothesis, density functional theory (DFT) simulations were performed to calculate the

https://doi.org/10.1021/jacsau.2c00635
JACS Au 2023, 3, 1337−1347

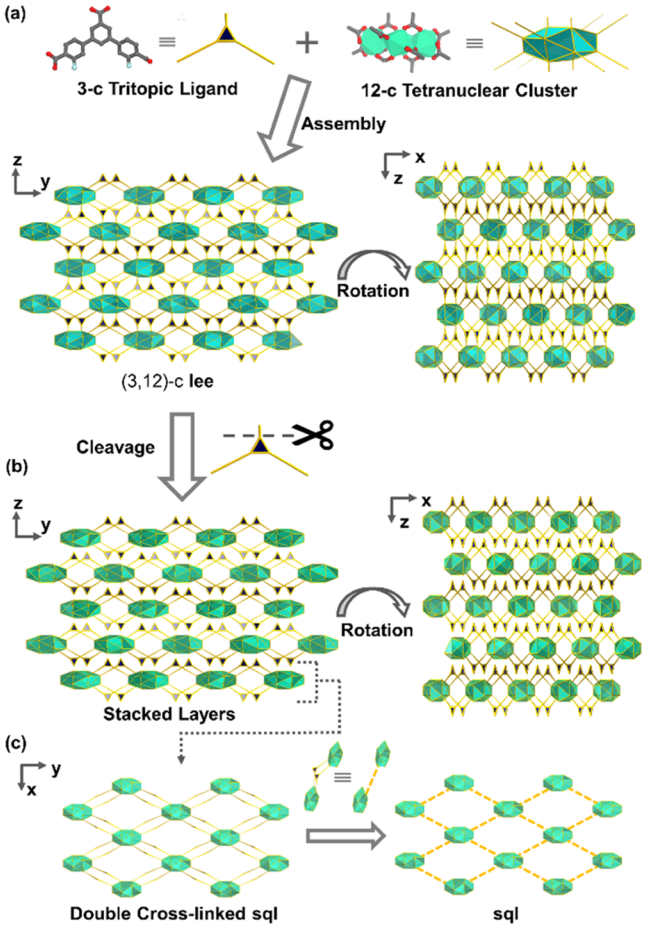

Figure 8. Structural illustration of PCN-993(Eu) featuring (3,12)-c **lee** topology. (a) lee net is based on the sphenomegacorona, representing a rare 12-c RE_4 cluster. (b) Close stack of the 12-c RE_4 clusters allows for the installation of H_3L-F to produce the layered structure. (c) Double cross-linked **sql** net is observed in the (3,12)-c **lee** net after the cleavage of one carboxylate of H_3L-F.

deprotonation free energies of the tricarboxylate ligands, which are negatively associated with acidity[92,93] (Figure S29). According to DFT calculations, the central carboxyl groups of H_3L-F and H_3L-CH_3 are more acidic than the peripheral ones, while the acidities of carboxyl groups are close in H_3L-Cl and H_3L-NH_2. Moreover, the acidity of central carboxyl of H_3L-OCH_3 is remarkably weaker than the peripheral ones due to the strong p-π electron donation from oxygen and the intramolecular hydrogen bonding. Herein, the calculation results demonstrate that the ortho functionalization of carboxylate groups enables the tuning of the acidity of tricarboxylate ligands.

SCXRD results reveal that the linkers feature various distorted conformations when confined in the frameworks (Tables S7 and S8). Single-point calculations were performed based upon the XRD-determined ligand geometries at B3LYP level. The ligand geometries were further optimized to attain the relaxation energy in the gas phase (Figures S31−S33). The energy changes were calculated by subtracting the free energy of the confined ligand with the one after geometry optimization. The calculation results showed that the ligands H_3L-Cl and H_3L-NH_2 feature close free energy changes around 50 kcal/mol after distortion, indicating that the two ligands have similar steric hindrances. Furthermore, the H_3L-CH_3 adopts three different conformations in PCN-991(Eu) with free energy changes of 62.92, 74.75, and 32.31 kcal/mol, respectively. Herein, the H_3L-CH_3 is distorted to accommodate the coexistence of RE_4 and RE_6 clusters. In addition, the fluoro-functionalized linker H_3L-F adopts different conformation in PCN-992(Eu) and PCN-993(Eu). The single-point energy of H_3L-F in PCN-993(Eu) is 21.9 kcal/mol lower than that in PCN-992(Eu). Such a significant energy difference demonstrates that PCN-993(Eu) is a thermodynamic product with a more stable ligand conformation.

The calculation results provide insights into the formation mechanism of RE MOFs. Likewise, the transformation from PCN-992(Eu) to PCN-993(Eu) is favored when considering the linker energy and higher connectivity number of the cluster. Herein, this MOF transformation can be dominated by the evolution of RE clusters during the synthesis, in which the RE_3 clusters are generated at the early synthetic stage to induce the occurrence of PCN-992(Eu). Due to the high coordination adaptivity of RE cations, the RE_3 cluster can be further extended into a 12-c RE_4 cluster, resulting in a more stable MOF PCN-993(Eu) with a decreased ligand conformational energy.

CONCLUSIONS

In conclusion, we present an ortho-functionalization strategy to alter the acidities and conformations of tricarboxylate linkers, which direct the formation of unexpected RE polynuclear clusters, including 8-c RE_3, 10-c RE_3, and 12-c RE_4. These novel building blocks led to the discovery of six MOFs named PCN-99*n* (*n* = 1−6) with unprecedented topologies. Furthermore, the utilization of H_3L-CH_3 functionalized with bulky methyl groups resulted in a (3,3,8,10)-c **kyw** net consisting of 8-c RE_4 and 10-c RE_6 clusters, while (3,3,3,10,10)-c **wxl**, (3,12)-c **gmx**, and (3,3,3,12)-c **joe** topologies were constructed based on RE_6 clusters with varying connectivity numbers. Interestingly, a phase transformation from a (3,8,10)-c **lfg** net to a (3,12)-c **lee** net was discovered, involving the displacement of RE_3 clusters with RE_4 clusters when extending the reaction time. This work unveils the significance of ortho effects in regulating the structures of organic ligand and RE polynuclear clusters, which will provide insights into the construction of framework materials with unprecedented structural complexity and application potentials.

ASSOCIATED CONTENT

Supporting Information

The Supporting Information is available free of charge at https://pubs.acs.org/doi/10.1021/jacsau.2c00635.

Synthetic procedures of all tricarboxylic linkers (Scheme S1−S5); crystal data and structure refinements for PCN-991(Eu) to PCN-996(Eu) (Tables S1 and S2); pK_a of ortho-substituted carboxylic acid (Figure S1, Tables S3−S6); structural illustrations of RE polynuclear clusters and MOFs (Figures S2−S7); power X-ray diffraction of MOFs (Figures S8−S14); thermal gravimetric analysis of MOFs (Figures S15−S19); Gas adsorption test of PCN-991(Eu) and PCN-996(Eu) (Figures S20−S26); optical images of MOF crystals (Figure S27); dihedral angle analysis of tritopic ligands in MOFs (Figure S28, Tables S7 and S8); computational calculation about ligand's energy and acidity (Figures S29−S33); ^1H

https://doi.org/10.1021/jacsau.2c00635
JACS Au 2023, 3, 1337−1347

NMR spectra of synthesized compounds (Figures S34–S44); ^{1}H NMR spectra of decomposed MOFs (Figures S45–S49) (PDF)

Accession Codes

X-ray crystallographic data for **PCN-99X** (X = 1-6) .The detailed crystallographic data can be obtained free of charge from The Cambridge Crystallographic Data Centre via www.ccdc.cam.ac.uk/data_request/cif (CCDC: 2122521-2122526).

AUTHOR INFORMATION

Corresponding Authors

Weidong Fan − *School of Materials Science and Engineering, College of Chemistry and Chemical Engineering, China University of Petroleum (East China), Qingdao, Shandong 266580, China;* orcid.org/0000-0002-7139-4137; Email: wdfan@upc.edu.cn

Daofeng Sun − *School of Materials Science and Engineering, College of Chemistry and Chemical Engineering, China University of Petroleum (East China), Qingdao, Shandong 266580, China;* orcid.org/0000-0003-3184-1841; Email: dfsun@upc.edu.cn

Hong-Cai Zhou − *Department of Chemistry, Texas A&M University, College Station, Texas 77843-3255, United States; Department of Materials Science and Engineering, Texas A&M University, College Station, Texas 77843-3255, United States;* orcid.org/0000-0002-9029-3788; Email: zhou@chem.tamu.edu

Authors

Fugang Li − *School of Materials Science and Engineering, College of Chemistry and Chemical Engineering, China University of Petroleum (East China), Qingdao, Shandong 266580, China*

Kun-Yu Wang − *Department of Chemistry, Texas A&M University, College Station, Texas 77843-3255, United States;* orcid.org/0000-0001-8982-0547

Zhengyang Liu − *School of Materials Science and Engineering, College of Chemistry and Chemical Engineering, China University of Petroleum (East China), Qingdao, Shandong 266580, China*

Zongsu Han − *Department of Chemistry, Texas A&M University, College Station, Texas 77843-3255, United States*

Dacheng Kuai − *Department of Chemistry, Texas A&M University, College Station, Texas 77843-3255, United States;* orcid.org/0000-0002-4787-7331

Liang Feng − *Department of Chemistry, Texas A&M University, College Station, Texas 77843-3255, United States*

Yutong Wang − *School of Materials Science and Engineering, College of Chemistry and Chemical Engineering, China University of Petroleum (East China), Qingdao, Shandong 266580, China;* orcid.org/0000-0001-8943-1832

Xiaokang Wang − *School of Materials Science and Engineering, College of Chemistry and Chemical Engineering, China University of Petroleum (East China), Qingdao, Shandong 266580, China*

Yue Li − *School of Materials Science and Engineering, College of Chemistry and Chemical Engineering, China University of Petroleum (East China), Qingdao, Shandong 266580, China*

Zhentao Yang − *Department of Chemistry, Texas A&M University, College Station, Texas 77843-3255, United States*

Rongming Wang − *School of Materials Science and Engineering, College of Chemistry and Chemical Engineering, China University of Petroleum (East China), Qingdao, Shandong 266580, China;* orcid.org/0000-0002-5445-541X

Complete contact information is available at: https://pubs.acs.org/10.1021/jacsau.2c00635

Author Contributions

[‖]F.L. and K.-Y.W. contributed equally. CRediT: **Fugang Li** data curation, methodology, project administration, resources, writing-original draft; **Kunyu Wang** conceptualization, data curation, formal analysis, methodology, resources, visualization, writing-review & editing; **Zhengyang Liu** data curation, investigation, resources; **Zongsu Han** data curation, investigation; **Dacheng Kuai** data curation, software; **Weidong Fan** conceptualization, funding acquisition, investigation, methodology, supervision; **Liang Feng** conceptualization, formal analysis, supervision; **Yutong Wang** data curation; **Xiaokang Wang** data curation, formal analysis, resources; **Yue Li** data curation, formal analysis, resources; **Zhentao Yang** formal analysis; **Rongming Wang** project administration, supervision; **Daofeng Sun** conceptualization, funding acquisition, supervision; **Hong-Cai Zhou** conceptualization, funding acquisition, investigation, supervision, validation.

Notes

The authors declare no competing financial interest.

ACKNOWLEDGMENTS

This work was supported by the National Natural Science Foundation of China (NSFC, Grant No. 22275210, 22201305), the Fundamental Research Funds for the Central Universities (22CX06024A), and the Outstanding Youth Science Fund Projects of Shandong Province (2022HWYQ-070). The authors also thank the support of the Robert A. Welch Foundation through a Welch Endowed Chair to H.-C.Z. (A-0030) and Qatar National Research Fund under Award Number NPRP9-377-1-080. The authors also acknowledge the support from the Foresight Institute.

REFERENCES

(1) Li, J.-R.; Kuppler, R. J.; Zhou, H.-C. Selective gas adsorption and separation in metal−organic frameworks. *Chem. Soc. Rev.* **2009**, *38*, 1477−1504.

(2) Li, J.-R.; Sculley, J.; Zhou, H.-C. Metal−Organic Frameworks for Separations. *Chem. Rev.* **2012**, *112*, 869−932.

(3) Bloch, E. D.; Queen Wendy, L.; Krishna, R.; Zadrozny Joseph, M.; Brown Craig, M.; Long Jeffrey, R. Hydrocarbon Separations in a Metal-Organic Framework with Open Iron(II) Coordination Sites. *Science* **2012**, *335*, 1606−1610.

(4) Cui, X.; Chen, K.; Xing, H.; Yang, Q.; Krishna, R.; Bao, Z.; Wu, H.; Zhou, W.; Dong, X.; Han, Y.; Li, B.; Ren, Q.; Zaworotko Michael, J.; Chen, B. Pore chemistry and size control in hybrid porous materials for acetylene capture from ethylene. *Science* **2016**, *353*, 141−144.

(5) Rosi, N. L.; Eckert, J.; Eddaoudi, M.; Vodak David, T.; Kim, J.; O'Keeffe, M.; Yaghi Omar, M. Hydrogen Storage in Microporous Metal-Organic Frameworks. *Science* **2003**, *300*, 1127−1129.

(6) Murray, L. J.; Dincă, M.; Long, J. R. Hydrogen storage in metal−organic frameworks. *Chem. Soc. Rev.* **2009**, *38*, 1294−1314.

(7) Mason, J. A.; Oktawiec, J.; Taylor, M. K.; Hudson, M. R.; Rodriguez, J.; Bachman, J. E.; Gonzalez, M. I.; Cervellino, A.; Guagliardi, A.; Brown, C. M.; Llewellyn, P. L.; Masciocchi, N.; Long,

J. R. Methane storage in flexible metal−organic frameworks with intrinsic thermal management. *Nature* **2015**, *527*, 357−361.
(8) He, Y.; Zhou, W.; Qian, G.; Chen, B. Methane storage in metal−organic frameworks. *Chem. Soc. Rev.* **2014**, *43*, 5657−5678.
(9) Chen, Z.; Li, P.; Anderson, R.; Wang, X.; Zhang, X.; Robison, L.; Redfern Louis, R.; Moribe, S.; Islamoglu, T.; Gómez-Gualdrón Diego, A.; Yildirim, T.; Stoddart, J. F.; Farha Omar, K. Balancing volumetric and gravimetric uptake in highly porous materials for clean energy. *Science* **2020**, *368*, 297−303.
(10) Liu, J.; Xie, D.; Shi, W.; Cheng, P. Coordination compounds in lithium storage and lithium-ion transport. *Chem. Soc. Rev.* **2020**, *49*, 1624−1642.
(11) Kim, H.; Yang, S.; Rao Sameer, R.; Narayanan, S.; Kapustin Eugene, A.; Furukawa, H.; Umans Ari, S.; Yaghi Omar, M.; Wang Evelyn, N. Water harvesting from air with metal-organic frameworks powered by natural sunlight. *Science* **2017**, *356*, 430−434.
(12) Xu, W.; Yaghi, O. M. Metal−Organic Frameworks for Water Harvesting from Air, Anywhere, Anytime. *ACS Cent. Sci.* **2020**, *6*, 1348−1354.
(13) Hanikel, N.; Pei, X.; Chheda, S.; Lyu, H.; Jeong, W.; Sauer, J.; Gagliardi, L.; Yaghi Omar, M. Evolution of water structures in metal-organic frameworks for improved atmospheric water harvesting. *Science* **2021**, *374*, 454−459.
(14) Millward, A. R.; Yaghi, O. M. Metal−Organic Frameworks with Exceptionally High Capacity for Storage of Carbon Dioxide at Room Temperature. *J. Am. Chem. Soc.* **2005**, *127*, 17998−17999.
(15) Banerjee, R.; Phan, A.; Wang, B.; Knobler, C.; Furukawa, H.; O'Keeffe, M.; Yaghi Omar, M. High-Throughput Synthesis of Zeolitic Imidazolate Frameworks and Application to CO2 Capture. *Science* **2008**, *319*, 939−943.
(16) Sumida, K.; Rogow, D. L.; Mason, J. A.; McDonald, T. M.; Bloch, E. D.; Herm, Z. R.; Bae, T.-H.; Long, J. R. Carbon Dioxide Capture in Metal−Organic Frameworks. *Chem. Rev.* **2012**, *112*, 724−781.
(17) D'Alessandro, D. M.; Smit, B.; Long, J. R. Carbon Dioxide Capture: Prospects for New Materials. *Angew. Chem., Int. Ed.* **2010**, *49*, 6058−6082.
(18) McDonald, T. M.; Mason, J. A.; Kong, X.; Bloch, E. D.; Gygi, D.; Dani, A.; Crocellà, V.; Giordanino, F.; Odoh, S. O.; Drisdell, W. S.; Vlaisavljevich, B.; Dzubak, A. L.; Poloni, R.; Schnell, S. K.; Planas, N.; Lee, K.; Pascal, T.; Wan, L. F.; Prendergast, D.; Neaton, J. B.; Smit, B.; Kortright, J. B.; Gagliardi, L.; Bordiga, S.; Reimer, J. A.; Long, J. R. Cooperative insertion of CO2 in diamine-appended metal-organic frameworks. *Nature* **2015**, *519*, 303−308.
(19) Yaghi, O. M.; Li, G.; Li, H. Selective binding and removal of guests in a microporous metal−organic framework. *Nature* **1995**, *378*, 703−706.
(20) Li, H.; Eddaoudi, M.; O'Keeffe, M.; Yaghi, O. M. Design and synthesis of an exceptionally stable and highly porous metal-organic framework. *Nature* **1999**, *402*, 276−279.
(21) Yaghi, O. M.; O'Keeffe, M.; Ockwig, N. W.; Chae, H. K.; Eddaoudi, M.; Kim, J. Reticular synthesis and the design of new materials. *Nature* **2003**, *423*, 705−714.
(22) O'Keeffe, M.; Yaghi, O. M. Deconstructing the Crystal Structures of Metal−Organic Frameworks and Related Materials into Their Underlying Nets. *Chem. Rev.* **2012**, *112*, 675−702.
(23) Zhou, H.-C.; Long, J. R.; Yaghi, O. M. Introduction to Metal−Organic Frameworks. *Chem. Rev.* **2012**, *112*, 673−674.
(24) Furukawa, H.; Cordova Kyle, E.; O'Keeffe, M.; Yaghi Omar, M. The Chemistry and Applications of Metal-Organic Frameworks. *Science* **2013**, *341*, No. 1230444.
(25) Zhou, H.-C. J.; Kitagawa, S. Metal−Organic Frameworks (MOFs). *Chem. Soc. Rev.* **2014**, *43*, 5415−5418.
(26) Guillerm, V.; Maspoch, D. Geometry Mismatch and Reticular Chemistry: Strategies To Assemble Metal−Organic Frameworks with Non-default Topologies. *J. Am. Chem. Soc.* **2019**, *141*, 16517−16538.
(27) Eddaoudi, M.; Kim, J.; O'Keeffe, M.; Yaghi, O. M. Cu2[o-Br-C6H3(CO2)2]2(H2O)2·(DMF)8(H2O)2: A Framework Deliberately Designed To Have the NbO Structure Type. *J. Am. Chem. Soc.* **2002**, *124*, 376−377.
(28) Furukawa, H.; Kim, J.; Ockwig, N. W.; O'Keeffe, M.; Yaghi, O. M. Control of Vertex Geometry, Structure Dimensionality, Functionality, and Pore Metrics in the Reticular Synthesis of Crystalline Metal−Organic Frameworks and Polyhedra. *J. Am. Chem. Soc.* **2008**, *130*, 11650−11661.
(29) Yuan, S.; Chen, Y.-P.; Qin, J.-S.; Lu, W.; Zou, L.; Zhang, Q.; Wang, X.; Sun, X.; Zhou, H.-C. Linker Installation: Engineering Pore Environment with Precisely Placed Functionalities in Zirconium MOFs. *J. Am. Chem. Soc.* **2016**, *138*, 8912−8919.
(30) Yuan, S.; Lu, W.; Chen, Y.-P.; Zhang, Q.; Liu, T.-F.; Feng, D.; Wang, X.; Qin, J.; Zhou, H.-C. Sequential Linker Installation: Precise Placement of Functional Groups in Multivariate Metal−Organic Frameworks. *J. Am. Chem. Soc.* **2015**, *137*, 3177−3180.
(31) Cavka, J. H.; Jakobsen, S.; Olsbye, U.; Guillou, N.; Lamberti, C.; Bordiga, S.; Lillerud, K. P.; New, A. A New Zirconium Inorganic Building Brick Forming Metal Organic Frameworks with Exceptional Stability. *J. Am. Chem. Soc.* **2008**, *130*, 13850−13851.
(32) Feng, L.; Day, G. S.; Wang, K.-Y.; Yuan, S.; Zhou, H.-C. Strategies for Pore Engineering in Zirconium Metal-Organic Frameworks. *Chem* **2020**, *6*, 2902−2923.
(33) Ejegbavwo, O. A.; Martin, C. R.; Olorunfemi, O. A.; Leith, G. A.; Ly, R. T.; Rice, A. M.; Dolgopolova, E. A.; Smith, M. D.; Karakalos, S. G.; Birkner, N.; Powell, B. A.; Pandey, S.; Koch, R. J.; Misture, S. T.; Loye, H.-C. z.; Phillpot, S. R.; Brinkman, K. S.; Shustova, N. B. Thermodynamics and Electronic Properties of Heterometallic Multinuclear Actinide-Containing Metal−Organic Frameworks with "Structural Memory. *J. Am. Chem. Soc.* **2019**, *141*, 11628−11640.
(34) Saraci, F.; Quezada-Novoa, V.; Donnarumma, P. R.; Howarth, A. J. Rare-earth metal−organic frameworks: from structure to applications. *Chem. Soc. Rev.* **2020**, *49*, 7949−7977.
(35) Zheng, Z. Ligand-controlled self-assembly of polynuclear lanthanide−oxo/hydroxo complexes: from synthetic serendipity to rational supramolecular design. *Chem. Commun.* **2001**, *24*, 2521−2529.
(36) Feng, L.; Pang, J.; She, P.; Li, J. L.; Qin, J. S.; Du, D. Y.; Zhou, H. C. Metal-Organic Frameworks Based on Group 3 and 4 Metals. *Adv. Mater.* **2020**, *32*, No. e2004414.
(37) Devic, T.; Serre, C.; Audebrand, N.; Marrot, J.; Férey, G. MIL-103, A 3-D Lanthanide-Based Metal Organic Framework with Large One-Dimensional Tunnels and A High Surface Area. *J. Am. Chem. Soc.* **2005**, *127*, 12788−12789.
(38) Luo, T.-Y.; Liu, C.; Eliseeva, S. V.; Muldoon, P. F.; Petoud, S.; Rosi, N. L. Rare Earth pcu Metal−Organic Framework Platform Based on RE4(μ3-OH)4(COO)62+ Clusters: Rational Design, Directed Synthesis, and Deliberate Tuning of Excitation Wavelengths. *J. Am. Chem. Soc.* **2017**, *139*, 9333−9340.
(39) Ma, B.-Q.; Zhang, D.-S.; Gao, S.; Jin, T.-Z.; Yan, C.-H.; Xu, G.-X. From Cubane to Supercubane: The Design, Synthesis, and Structure of a Three-Dimensional Open Framework Based on a Ln4O4 Cluster. *Angew. Chem., Int. Ed.* **2000**, *39*, 3644−3646.
(40) Wang, R.; Liu, H.; Carducci, M. D.; Jin, T.; Zheng, C.; Zheng, Z. Lanthanide Coordination with α-Amino Acids under Near Physiological pH Conditions: Polymetallic Complexes Containing the Cubane-Like [Ln4(μ3-OH)4]8+ Cluster Core. *Inorg. Chem.* **2001**, *40*, 2743−2750.
(41) Gao, Y.; Xu, G.-F.; Zhao, L.; Tang, J.; Liu, Z. Observation of Slow Magnetic Relaxation in Discrete Dysprosium Cubane. *Inorg. Chem.* **2009**, *48*, 11495−11497.
(42) Lin, P.-H.; Korobkov, I.; Wernsdorfer, W.; Ungur, L.; Chibotaru, L. F.; Murugesu, M. A Rare μ4-O Centred Dy4 Tetrahedron with Coordination-Induced Local Chirality and Single-Molecule Magnet Behaviour. *Eur. J. Inorg. Chem.* **2011**, *2011*, 1535−1539.
(43) Yi, X.; Bernot, K.; Calvez, G.; Daiguebonne, C.; Guillou, O. 3D Organization of Dysprosium Cubanes. *Eur. J. Inorg. Chem.* **2013**, *2013*, 5879−5885.

https://doi.org/10.1021/jacsau.2c00635
JACS Au 2023, 3, 1337−1347

(44) Zhou, J.-M.; Shi, W.; Li, H.-M.; Li, H.; Cheng, P. Experimental Studies and Mechanism Analysis of High-Sensitivity Luminescent Sensing of Pollutional Small Molecules and Ions in Ln4O4 Cluster Based Microporous Metal−Organic Frameworks. *J. Phys. Chem. C* **2014**, *118*, 416−426.
(45) Zou, D.; Zhang, J.; Cui, Y.; Qian, G. Near-infrared-emissive metal−organic frameworks. *Dalton Trans.* **2019**, *48*, 6669−6675.
(46) Maruyama, T.; Kawabata, H.; Kikukawa, Y.; Hayashi, Y. Yttrium-Containing Sandwich-, Ring-, and Cage-Type Polyoxovanadates: Synthesis and Characterization. *Eur. J. Inorg. Chem.* **2019**, *2019*, 529−533.
(47) Litvinova, Y. M.; Gayfulin, Y. M.; van Leusen, J.; Samsonenko, D. G.; Lazarenko, V. A.; Zubavichus, Y. V.; Kögerler, P.; Mironov, Y. V. Metal−organic frameworks based on polynuclear lanthanide complexes and octahedral rhenium clusters. *Inorg. Chem. Front.* **2019**, *6*, 1518−1526.
(48) Xue, D.-X.; Cairns, A. J.; Belmabkhout, Y.; Wojtas, L.; Liu, Y.; Alkordi, M. H.; Eddaoudi, M. Tunable Rare-Earth fcu-MOFs: A Platform for Systematic Enhancement of CO2 Adsorption Energetics and Uptake. *J. Am. Chem. Soc.* **2013**, *135*, 7660−7667.
(49) Alezi, D.; Peedikakkal, A. M. P.; Weseliński, ŁJ.; Guillerm, V.; Belmabkhout, Y.; Cairns, A. J.; Chen, Z.; Wojtas, Ł.; Eddaoudi, M. Quest for Highly Connected Metal−Organic Framework Platforms: Rare-Earth Polynuclear Clusters Versatility Meets Net Topology Needs. *J. Am. Chem. Soc.* **2015**, *137*, 5421−5430.
(50) Wang, Y.; Feng, L.; Fan, W.; Wang, K.-Y.; Wang, X.; Wang, X.; Zhang, K.; Zhang, X.; Dai, F.; Sun, D.; Zhou, H.-C. Topology Exploration in Highly Connected Rare-Earth Metal−Organic Frameworks via Continuous Hindrance Control. *J. Am. Chem. Soc.* **2019**, *141*, 6967−6975.
(51) Lin, S.-k.; March, J. March's Advanced Organic Chemistry: Reactions, Mechanisms, and Structure, 5th Edition. *Molecules* **2001**, *6*, No. 1064.
(52) Böhm, S.; Fiedler, P.; Exner, O. Analysis of the ortho effect: acidity of 2-substituted benzoic acids. *New J. Chem.* **2004**, *28*, 67−74.
(53) Chen, L.; Hu, H.-J.; Wang, Y.-L.; Zhang, X.-F.; Xu, L.-P.; Liu, Q.-Y. Metal−Organic Frameworks Featuring 18-Connected Nonanuclear Rare-Earth Oxygen Clusters and Cavities for Efficient C2H2/CO2 Separation. *Inorg. Chem.* **2021**, *60*, 13471−13478.
(54) Guillerm, V.; Weseliński, ŁJ.; Belmabkhout, Y.; Cairns, A. J.; D'Elia, V.; Wojtas, Ł.; Adil, K.; Eddaoudi, M. Discovery and introduction of a (3,18)-connected net as an ideal blueprint for the design of metal−organic frameworks. *Nat. Chem.* **2014**, *6*, 673−680.
(55) Lin, W.; Ning, E.; Yang, L.; Rao, Y.; Peng, S.; Li, Q. Snapshots of Postsynthetic Modification in a Layered Metal−Organic Framework: Isometric Linker Exchange and Adaptive Linker Installation. *Inorg. Chem.* **2021**, *60*, 11756−11763.
(56) Mahé, N.; Guillou, O.; Daiguebonne, C.; Gérault, Y.; Caneschi, A.; Sangregorio, C.; Chane-Ching, J. Y.; Car, P. E.; Roisnel, T. Polynuclear Lanthanide Hydroxo Complexes: New Chemical Precursors for Coordination Polymers. *Inorg. Chem.* **2005**, *44*, 7743−7750.
(57) Savard, D.; Lin, P.-H.; Burchell, T. J.; Korobkov, I.; Wernsdorfer, W.; Clérac, R.; Murugesu, M. Two-Dimensional Networks of Lanthanide Cubane-Shaped Dumbbells. *Inorg. Chem.* **2009**, *48*, 11748−11754.
(58) Wang, R.; Carducci, M. D.; Zheng, Z. Direct Hydrolytic Route to Molecular Oxo−Hydroxo Lanthanide Clusters. *Inorg. Chem.* **2000**, *39*, 1836−1837.
(59) Blatov, V. A.; Shevchenko, A. P.; Proserpio, D. M. Applied Topological Analysis of Crystal Structures with the Program Package ToposPro. *Cryst. Growth Des.* **2014**, *14*, 3576−3586.
(60) Blatov, V. A. *Multipurpose Crystallochemical Analysis with the Program Package TOPOS*, IUCr CompComm Newsletter, 2006; pp 4−38.
(61) Guillerm, V.; Eddaoudi, M. The Importance of Highly Connected Building Units in Reticular Chemistry: Thoughtful Design of Metal−Organic Frameworks. *Acc. Chem. Res.* **2021**, *54*, 3298−3312.
(62) Férey, G.; Serre, C.; Mellot-Draznieks, C.; Millange, F.; Surblé, S.; Dutour, J.; Margiolaki, I. A Hybrid Solid with Giant Pores Prepared by a Combination of Targeted Chemistry, Simulation, and Powder Diffraction. *Angew. Chem., Int. Ed.* **2004**, *43*, 6296−6301.
(63) Férey, G.; Mellot-Draznieks, C.; Serre, C.; Millange, F.; Dutour, J.; Surblé, S.; Margiolaki, I. A Chromium Terephthalate-Based Solid with Unusually Large Pore Volumes and Surface Area. *Science* **2005**, *309*, 2040−2042.
(64) Serre, C.; Mellot-Draznieks, C.; Surblé, S.; Audebrand, N.; Filinchuk, Y.; Férey, G. Role of Solvent-Host Interactions That Lead to Very Large Swelling of Hybrid Frameworks. *Science* **2007**, *315*, 1828−1831.
(65) Horcajada, P.; Surblé, S.; Serre, C.; Hong, D.-Y.; Seo, Y.-K.; Chang, J.-S.; Grenèche, J.-M.; Margiolaki, I.; Férey, G. Synthesis and catalytic properties of MIL-100(Fe), an iron(iii) carboxylate with large pores. *Chem. Commun.* **2007**, *27*, 2820−2822.
(66) Chen, Z.; Li, P.; Zhang, X.; Li, P.; Wasson, M. C.; Islamoglu, T.; Stoddart, J. F.; Farha, O. K. Reticular Access to Highly Porous acs-MOFs with Rigid Trigonal Prismatic Linkers for Water Sorption. *J. Am. Chem. Soc.* **2019**, *141*, 2900−2905.
(67) Feng, D.; Wang, K.; Wei, Z.; Chen, Y.-P.; Simon, C. M.; Arvapally, R. K.; Martin, R. L.; Bosch, M.; Liu, T.-F.; Fordham, S.; Yuan, D.; Omary, M. A.; Haranczyk, M.; Smit, B.; Zhou, H.-C. Kinetically tuned dimensional augmentation as a versatile synthetic route towards robust metal−organic frameworks. *Nat. Commun.* **2014**, *5*, No. 5723.
(68) Bhattacharjee, S.; Chen, C.; Ahn, W.-S. Chromium terephthalate metal−organic framework MIL-101: synthesis, functionalization, and applications for adsorption and catalysis. *RSC Adv.* **2014**, *4*, 52500−52525.
(69) Lian, X.; Chen, Y.-P.; Liu, T.-F.; Zhou, H.-C. Coupling two enzymes into a tandem nanoreactor utilizing a hierarchically structured MOF. *Chem. Sci.* **2016**, *7*, 6969−6973.
(70) Dezotti, Y.; Ribeiro, M. A.; Pirota, K. R.; Barros, W. P. Influence of the Metal Ion on the Topology and Interpenetration of Pyridylvinyl(benzoate) Based Metal−Organic Frameworks. *Cryst. Growth Des.* **2019**, *19*, 5592−5603.
(71) Ma, G.; Zhang, J.-J.; Sun, L.; Xu, Y.-X.; Gao, H.-L.; Zhang, H.-Y.; He, X.-W. A New Cluster-Based MOF for Selective Gas Sorption and Treatment Effect on Acute glomerulonephritis by Reducing NF-κb Pathway Activation and Cytokines Release. *J. Cluster Sci.* **2020**, *31*, 1061−1069.
(72) Chen, X.-Y.; Zhao, B.; Shi, W.; Xia, J.; Cheng, P.; Liao, D.-Z.; Yan, S.-P.; Jiang, Z.-H. Microporous Metal−Organic Frameworks Built on a Ln3 Cluster as a Six-Connecting Node. *Chem. Mater.* **2005**, *17*, 2866−2874.
(73) Karmakar, A.; Hazra, S.; Guedes da Silva, M. F. C.; Paul, A.; Pombeiro, A. J. L. Nanoporous lanthanide metal−organic frameworks as efficient heterogeneous catalysts for the Henry reaction. *CrystEngComm* **2016**, *18*, 1337−1349.
(74) Liu, B.; Wu, W.-P.; Hou, L.; Wang, Y.-Y. Four uncommon nanocage-based Ln-MOFs: highly selective luminescent sensing for Cu2+ ions and selective CO2 capture. *Chem. Commun.* **2014**, *50*, 8731−8734.
(75) Zhang, L.; Song, T.; Xu, J.; Sun, J.; Zeng, S.; Wu, Y.; Fan, Y.; Wang, L. Polymorphic Ln(iii) and BPTC-based porous metal−organic frameworks with visible, NIR photoluminescent and magnetic properties. *CrystEngComm* **2014**, *16*, 2440−2451.
(76) Xu, H.; Fang, M.; Cao, C.-S.; Qiao, W.-Z.; Zhao, B. Unique (3,4,10)-Connected Lanthanide−Organic Framework as a Recyclable Chemical Sensor for Detecting Al3. *Inorg. Chem.* **2016**, *55*, 4790−4794.
(77) Li, Y.-J.; Wang, Y.-L.; Liu, Q.-Y. The Highly Connected MOFs Constructed from Nonanuclear and Trinuclear Lanthanide-Carboxylate Clusters: Selective Gas Adsorption and Luminescent pH Sensing. *Inorg. Chem.* **2017**, *56*, 2159−2164.
(78) Wei, N.; Zuo, R.-X.; Zhang, Y.-Y.; Han, Z.-B.; Gu, X.-J. Robust high-connected rare-earth MOFs as efficient heterogeneous catalysts for CO2 conversion. *Chem. Commun.* **2017**, *53*, 3224−3227.

https://doi.org/10.1021/jacsau.2c00635
JACS Au 2023, 3, 1337−1347

(79) Evans, W. J.; Sollberger, M. S. Synthetic and structural studies on the formation of a tetradecametallic yttrium oxide alkoxide chloride complex: an example of how molecular yttrium oxygen frameworks form extended arrays. *Inorg. Chem.* **1988**, *27*, 4417−4423.
(80) Wong, K.-L.; Zhu, Y.-M.; Yang, Y.-Y.; Law, G.-L.; Fan, H.-H.; Tanner, P. A.; Wong, W.-T. Structure and photophysical properties of new trinuclear lanthanide complexes (Ln=Eu and Tb) with 1,10-phenanthroline. *Inorg. Chem. Commun.* **2009**, *12*, 52−54.
(81) Paluch, M.; Ślepokura, K.; Lis, T.; Lisowski, J. Enantiopure trinuclear lanthanide(III) complexes: Cooperative formation of Ln3(μ3-OH)2 core within the macrocycle. *Inorg. Chem. Commun.* **2011**, *14*, 92−95.
(82) Costes, J.-P.; Dahan, F.; Nicodème, F.; Trinuclear, A. Gadolinium Complex: Structure and Magnetic Properties. *Inorg. Chem.* **2001**, *40*, 5285−5287.
(83) Xue, S.; Chen, X.-H.; Zhao, L.; Guo, Y.-N.; Tang, J. Two Bulky-Decorated Triangular Dysprosium Aggregates Conserving Vortex-Spin Structure. *Inorg. Chem.* **2012**, *51*, 13264−13270.
(84) Kobyłka, M. J.; Ślepokura, K.; Acebrón Rodicio, M.; Paluch, M.; Lisowski, J. Incorporation of Trinuclear Lanthanide(III) Hydroxo Bridged Clusters in Macrocyclic Frameworks. *Inorg. Chem.* **2013**, *52*, 12893−12903.
(85) Barash, E. H.; Coan, P. S.; Lobkovsky, E. B.; Streib, W. E.; Caulton, K. G. Anhydrous yttrium acetylacetonate and the course of thermal "dehydration" of Y(acac)3.3H2O. *Inorg. Chem.* **1993**, *32*, 497−501.
(86) Ma, S.; Yuan, D.; Wang, X.-S.; Zhou, H.-C. Microporous Lanthanide Metal-Organic Frameworks Containing Coordinatively Linked Interpenetration: Syntheses, Gas Adsorption Studies, Thermal Stability Analysis, and Photoluminescence Investigation. *Inorg. Chem.* **2009**, *48*, 2072−2077.
(87) Han, L.; Zhang, S.; Wang, Y.; Yan, X.; Lu, X. A Strategy for Synthesis of Ionic Metal-Organic Frameworks. *Inorg. Chem.* **2009**, *48*, 786−788.
(88) Wang, R.; Selby, H. D.; Liu, H.; Carducci, M. D.; Jin, T.; Zheng, Z.; Anthis, J. W.; Staples, R. J. Halide-Templated Assembly of Polynuclear Lanthanide-Hydroxo Complexes. *Inorg. Chem.* **2002**, *41*, 278−286.
(89) Kong, X.-J.; Long, L.-S.; Zheng, L.-S.; Wang, R.; Zheng, Z. Hydrolytic Synthesis and Structural Characterization of Lanthanide Hydroxide Clusters Supported by Nicotinic Acid. *Inorg. Chem.* **2009**, *48*, 3268−3273.
(90) Wu, Y.; Morton, S.; Kong, X.; Nichol, G. S.; Zheng, Z. Hydrolytic synthesis and structural characterization of lanthanide-acetylacetonato/hydroxo cluster complexes − A systematic study. *Dalton Trans.* **2011**, *40*, 1041−1046.
(91) Zheng, X.-Y.; Kong, X.-J.; Zheng, Z.; Long, L.-S.; Zheng, L.-S. High-Nuclearity Lanthanide-Containing Clusters as Potential Molecular Magnetic Coolers. *Acc. Chem. Res.* **2018**, *51*, 517−525.
(92) Bodnarchuk, M. S.; Heyes, D. M.; Dini, D.; Chahine, S.; Edwards, S. Role of Deprotonation Free Energies in pKa Prediction and Molecule Ranking. *J. Chem. Theory Comput.* **2014**, *10*, 2537−2545.
(93) Williams, S. L.; de Oliveira, C. A. F.; McCammon, J. A. Coupling Constant pH Molecular Dynamics with Accelerated Molecular Dynamics. *J. Chem. Theory Comput.* **2010**, *6*, 560−568.

https://doi.org/10.1021/jacsau.2c00635
JACS Au 2023, 3, 1337−1347